SCIENCE CHINA
Life Sciences

•RESEARCH PAPER•

https://doi.org/10.1007/s11427-022-2328-x

# Endothelial extracellular vesicles induce acute lung injury via follistatin-like protein 1

Hao-Xiang Yuan[1,2†], Ya-Ting Chen[1,2†], Yu-Quan Li[1,2†], Yan-Sheng Wang[5,6,7†], Zhi-Jun Ou[2,3†], Yan Li[1,2†], Jian-Jun Gao[1,2], Meng-Jie Deng[1,2], Yuan-Kai Song[1,2], Li Fu[1,2], Hong-Bo Ci[1,2], Feng-Jun Chang[1,2], Yang Cao[1,2], Yu-Peng Jian[1,2], Bi-Ang Kang[1,2], Zhi-Wei Mo[1,2], Da-Sheng Ning[1,2], Yue-Ming Peng[1,2], Ze-Long Liu[1,2], Xiao-Jun Liu[1,2], Ying-Qi Xu[1,2], Jun Xu[5,6,7*] & Jing-Song Ou[1,2,4*]

[1]*Division of Cardiac Surgery, Cardiovascular Diseases Institute, The First Affiliated Hospital, Sun Yat-sen University, Guangzhou 510080, China;*
[2]*National-Guangdong Joint Engineering Laboratory for Diagnosis and Treatment of Vascular Diseases, NHC Key Laboratory of Assisted Circulation (Sun Yat-sen University), Guangdong Provincial Engineering and Technology Center for Diagnosis and Treatment of Vascular Diseases, Guangzhou 510080, China;*
[3]*Division of Hypertension and Vascular Diseases, Cardiovascular Diseases Institute, The First Affiliated Hospital, Sun Yat-sen University, Guangzhou 510080, China;*
[4]*Guangdong Provincial Key Laboratory of Brain Function and Disease, Guangzhou 510080, China;*
[5]*State Key Laboratory of Respiratory Disease, Guangzhou 510120, China;*
[6]*Guangzhou Institute of Respiratory Health, Guangzhou 510120, China;*
[7]*The First Affiliated Hospital of Guangzhou Medical University, Guangzhou 510120, China*

Received September 12, 2022; accepted March 6, 2023; published online May 17, 2023

Cardiopulmonary bypass has been speculated to elicit systemic inflammation to initiate acute lung injury (ALI), including acute respiratory distress syndrome (ARDS), in patients after cardiac surgery. We previously found that post-operative patients showed an increase in endothelial cell-derived extracellular vesicles (eEVs) with components of coagulation and acute inflammatory responses. However, the mechanism underlying the onset of ALI owing to the release of eEVs after cardiopulmonary bypass, remains unclear. Plasma plasminogen-activated inhibitor-1 (PAI-1) and eEV levels were measured in patients with cardiopulmonary bypass. Endothelial cells and mice (C57BL/6, Toll-like receptor 4 knockout ($TLR4^{-/-}$) and inducible nitric oxide synthase knockout ($iNOS^{-/-}$)) were challenged with eEVs isolated from PAI-1-stimulated endothelial cells. Plasma PAI-1 and eEVs were remarkably enhanced after cardiopulmonary bypass. Plasma PAI-1 elevation was positively correlated with the increase in eEVs. The increase in plasma PAI-1 and eEV levels was associated with post-operative ARDS. The eEVs derived from PAI-1-stimulated endothelial cells could recognize TLR4 to stimulate a downstream signaling cascade identified as the Janus kinase 2/3 (JAK2/3)-signal transducer and activator of transcription 3 (STAT3)-interferon regulatory factor 1 (IRF-1) pathway, along with iNOS induction, and cytokine/chemokine production in vascular endothelial cells and C57BL/6 mice, ultimately contributing to ALI. ALI could be attenuated by JAK2/3 or STAT3 inhibitors (AG490 or S3I-201, respectively), and was relieved in $TLR4^{-/-}$ and $iNOS^{-/-}$ mice. eEVs activate the TLR4/JAK3/STAT3/IRF-1 signaling pathway to induce ALI/ARDS by delivering follistatin-like protein 1 (FSTL1), and FSTL1 knockdown in eEVs alleviates eEV-induced ALI/ARDS. Our data thus demonstrate that cardiopulmonary bypass may increase plasma PAI-1 levels to induce FSTL1-enriched eEVs, which target the TLR4-mediated JAK2/3/STAT3/IRF-1 signaling cascade and form a positive feedback loop, leading to ALI/ARDS after cardiac surgery. Our findings provide new insight into the molecular mechanisms and therapeutic targets for ALI/ARDS after cardiac surgery.

†Contributed equally to this work
*Corresponding authors (Jun Xu, email:wolaorenjia@vip.sina.com; Jing-Song Ou, email: oujs@mail.sysu.edu.cn)

**cell-derived extracellular vesicles, acute lung injury, acute respiratory distress syndrome, cardiopulmonary bypass, follistatin-like protein 1**

**Citation:** Yuan, H.X., Chen, Y.T., Li, Y.Q., Wang, Y.S., Ou, Z.J., Li, Y., Gao, J.J., Deng, M.J., Song, Y.K., Fu, L., et al. (2023). Endothelial extracellular vesicles induce acute lung injury via follistatin-like protein 1. Sci China Life Sci 66, https://doi.org/10.1007/s11427-022-2328-x

## INTRODUCTION

Acute respiratory distress syndrome (ARDS) is a potentially life-threatening complication in patients undergoing cardiac surgery. Cardiopulmonary bypass (CPB) is speculated to elicit a systemic inflammatory response that could, at least partially, explain ARDS onset in patients undergoing cardiac surgery. However, the pathophysiology of ARDS occurrence after CPB remains to be completely defined (Kwak et al., 2021; Sandeep et al., 2022).

Plasminogen-activated inhibitor-1 (PAI-1) is an important component of coagulation. Turbulence in PAI-1 levels tilts the balance of the hemostatic system, resulting in bleeding or thrombotic complications (Sandeep et al., 2022). Elevated PAI-1 levels have been associated with increased ARDS risk in patients undergoing cardiac surgery (Yadav et al., 2018). A recent discovery of a coalition between the hemostatic and inflammatory pathways has exposed a distinct role for PAI-1 (Coats and Morsy, 2020; Tipoe et al., 2018; Yadav et al., 2018).

Vascular endothelial cell-derived extracellular vesicles (eEVs) play crucial roles in intercellular communication, both in regulating homeostasis and in the pathogenesis of various diseases (Qi et al., 2021). Indeed, eEVs are elevated in the plasma of patients with ARDS compared with that in healthy controls or in patients with cardiogenic pulmonary edema (Densmore et al., 2006; Fujimoto et al., 2020; Ou et al., 2011; Yuan et al., 2020). We have previously revealed differential protein components enclosed in circulating microparticles (MPs), also called extracellular vesicles (EVs), from patients with valvular heart disease (VHD) before and after undergoing CPB (Ci et al., 2013; Jian et al., 2019; Lin et al., 2017; Ma et al., 2021; Song et al., 2022). Further, the unique proteins in post-operative MPs are primarily involved in coagulation, indicating an important relationship between PAI-1 and specific eEVs in the development of systemic inflammatory reactions, with respect to ensuing ARDS in patients after CPB.

Vascular endothelial cells (ECs) express an array of immune receptors that respond to harmful factors. Toll-like receptor 4 (TLR4) is a well-known critical transmembrane immune receptor mainly located in the cytomembrane. TLR4 recognizes the classical agonist lipopolysaccharide (Kim et al., 2022) as well as damage-associated molecular patterns (DAMPs) (Shirey et al., 2021), and triggers downstream signaling pathways that induce inflammatory cytokine release, leading to tissue damage. Recent studies have provided evidence that DAMPs are present in eEVs (Andres et al., 2020; Peterson et al., 2008; Sander et al., 2008). To date, it remains unclear whether elevated PAI-1 during CPB stimulates the secretion of eEVs (Chen et al., 2020; Jian et al., 2019; Li et al., 2021; Peterson et al., 2008; Sander et al., 2008; Yuan et al., 2022) attributable to the entry of DAMPs into systemic circulation, booting a secondary immune inflammatory response in the lungs.

The present study aimed to address the association between hemostatic and inflammatory pathways in acute lung injury (ALI) in relation to cardiac surgery with CPB. We verify for the first time that elevated plasma PAI-1 in patients undergoing cardiac surgery with CPB may stimulate the secretion of specific eEVs that bind to TLR4 via transported follistatin-like protein 1 (FSTL1), resulting in the activation of janus kinase/signal transducer and activator of transcription (JAK/STAT)/interferon regulatory factor 1 (IRF-1) signaling for a "second-hit," thus contributing to ALI.

## RESULTS

### eEV elevation induces ARDS after cardiac surgery with CPB through activation of TLR4 signaling

We compared the levels of plasma PAI-1 and circulating eEVs collected from enrolled patients before and 12 h after cardiac surgery with CPB. A high-sensitivity flow cytometer with a standardization experiment using size-calibrated beads was used to set the eEVs gates and quantify circulating eEVs (Figure S1A–D in Supporting Information). We detected significantly increased levels of both PAI-1 and eEVs in patients after CPB (Figure 1A and B). Plasma PAI-1 levels increased with the time taken for CPB in the patients, along with lower oxygenation index (OI) levels (Figure S2 in Supporting Information). The higher the plasma PAI-1 level, the higher the number of eEVs, and an increase in eEVs was closely correlated with a decreased OI (Figure 1C and D). Based on the Berlin definition, 12 of the 40 recruited patients (12/40) undergoing cardiac surgery with CPB were diagnosed with ARDS after surgery (Table S1 in Supporting Information). Post-operative patients with ARDS showed much higher levels of both PAI-1 and eEVs than those in patients without ARDS (Figure 1E and F).

Next, we isolated eEVs from cultured human umbilical vein endothelial cells (HUVECs) stimulated with PAI-1. The flow cytometric detection strategy for eEVs is described in Figure S1E and F in the Supporting Information. eEVs were

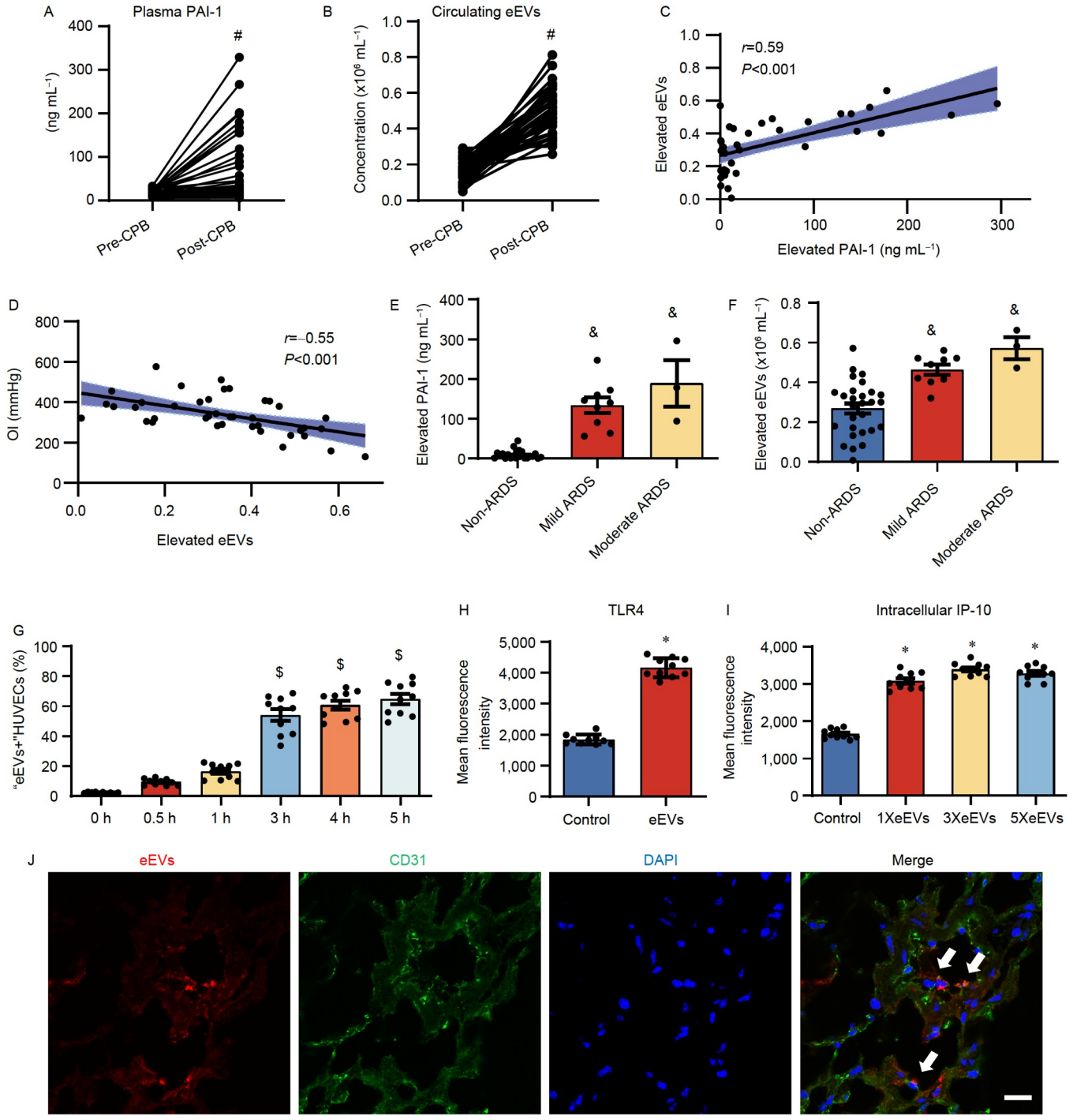


**Figure 1** Effect of elevated eEVs after CPB on post-operative ARDS in cardiac surgery patients. A and B, Patients with heart disease undergoing cardiac surgery with CPB were enrolled. Blood was drawn before cardiac surgery (Pre-CPB) and 12 h after cardiac surgery (Post-CPB) to detect the concentrations of PAI-1 and circulating eEVs. Dot plots show the changes in plasma PAI-1 and circulating eEVs before and after cardiac surgery with CPB. C, Correlation between elevation of PAI-1 and eEVs in patients after cardiac surgery with CPB was calculated using Spearman's correlation analysis. D, Correlation between elevation of eEVs and OI post-CPB was evaluated using Spearman's correlation analysis. E and F, Patients were further divided into mild ARDS, moderate ARDS, and non-ARDS groups after cardiac surgery. The dot plots show changes in the elevation of PAI-1 and eEVs after cardiac surgery with CPB. G, HUVECs were incubated with CD144-labeled eEVs for different times and "eEVs+" HUVECs are represented in the dot plots. H and I, Fluorescence values of TLR4 and IP-10 in HUVECs after eEV exposure. J, Immunofluorescence staining in lung sections of C57BL/6 wild type (C57) mice 6 h after intravenous injection of PKH26-labeled eEVs (red), showing PKH26-labeled eEVs adhesion on capillaries in the lung (white arrow). CD31 antibody (green) was used to stain endothelial cells and DAPI (blue) was to label cell nuclei in the lung sections. All data represent the mean and SEM of independent experiments. Statistical analysis was performed using the compared *t*-test for panels A and B, *t*-test for panel H, and one-way ANOVA with Tukey's test for panels E–G and I. Scale bars: 10 μm, 1× eEVs ($1\times10^5$ mL$^{-1}$); 3×eEVs ($3\times10^5$ mL$^{-1}$), and 5×eEVs ($5\times10^5$ mL$^{-1}$). $ *vs*. 0 H; * *vs*. control; # *vs*. Pre-CPB; & *vs*. non-ARDS. $P<0.05$, $n=10$.

characterized by electron microscopy, nanoparticle tracking analysis, and the expression of EV biomarkers (Figure S3 in Supporting Information). eEVs labeled with PKH26 could be absorbed by HUVECs (Figure S4 in Supporting Information). Following the addition of labeled eEVs to cultured HUVECs, flow cytometry and immune fluorescence assays showed an enhanced number of ECs combined with eEVs in a time-dependent manner, peaking at 4 h after exposure to eEVs (Figure 1G; Figure S5A in Supporting Information), while the rate of TLR4-positive HUVECs increased along with intracellular interferon-γ-inducible protein-10 (IP-10) production (Figure 1H and I; Figure S5B and C in Supporting Information). *In vivo*, after intravenous injection of PKH26-labeled eEVs into C57BL/6 wild-type mice, the number of eEVs in the mouse plasma rapidly increased, peaking at 15 min and declining after 1 h (Figure S6 in Supporting Information). An immunofluorescence assay of the lung tissue sections showed that the eEVs could bind to the pulmonary capillary endothelium (Figure 1J).

## eEVs trigger TLR4-mediated JAK3/STAT3/IRF-1 signal pathway and initiate inflammatory responses in vascular ECs

We cultured HUVECs under eEV stimulation and found that eEVs induced the activation of JAK2/3 and STAT3 phosphorylation *in vitro* (Figure S7 in Supporting Information). Addition of silencing RNA targeting TLR4 (Si-TLR4) downregulated TLR4 overexpression in HUVECs exposed to eEVs (Figure 2A and B; Figure S8 in Supporting Information), accompanied by blockade of JAK3/STAT3 phosphorylation and IRF-1 expression (Figure 2C; Figure S9 in Supporting Information). Similar to Si-TLR4 addition prior to the stimulation of eEVs in ECs, pretreatment with either AG490 or S3I-201 (inhibitors of JAK (JAK2/3) and STAT3, respectively) resulted in inhibition of JAK2/3 or STAT3 phosphorylation and reduction of IRF-1 transcription followed by abrogation of inducible nitric oxide synthase (iNOS) induction (Figure 2D and E; Figure S10 in Supporting Information). The addition of AG490 or S3I-201 also blocked cytokine/chemokine production in HUVECs in response to eEVs (Figure 2F).

## eEVs added to systemic circulation induce acute lung injury in the C57 mice

We further explored the relationship between systemic circulating eEVs and ALI induction *in vivo*. TLR4$^{-/-}$, inducible nitic oxide synthase knockout (iNOS$^{-/-}$), and C57BL/6 wild-type (C57) mice were injected intravenously with eEVs. Micro-computed tomography (micro-CT) scanning and pulmonary pathologic examination demonstrated that ALI, which represents pulmonary inflammation effusion, immune cell aggregation, and interstitial edema, was induced by circulating eEVs in wild-type mice (Figure 3A and B), and was attenuated in TLR4$^{-/-}$ (Figure 3A and B) and iNOS$^{-/-}$ mice (Figure 3C and D), or in wild-type mice pretreated with either AG490 or S3I-201 prior to the addition of eEVs (Figure 3E). Further immunohistochemistry (IHC) staining also demonstrated that eEVs-induced pulmonary accumulation of immune cells, including neutrophils and macrophages, was reduced in TLR4$^{-/-}$ (Figure S11 in Supporting Information) and iNOS$^{-/-}$ mice (Figure S12 in Supporting Information), or in C57 wild-type mice pretreated with either AG490 or S3I-201 prior to the addition of eEVs (Figure S13 in Supporting Information). eEVs reduced the percutaneous oxygen saturation ($SpO_2$) and partial pressure of arterial oxygen ($PaO_2$); further, the decrease in $SpO_2$ and $PaO_2$ induced by eEVs was mild in TLR4$^{-/-}$ mice, iNOS$^{-/-}$ mice and C57BL/6 wild-type mice pretreated with either AG490 or S3I-201 (Figure 3F–I).

## eEVs induce ALI in C57 mice through JAK2/3/STAT3/IRF-1/iNOS signaling

To define the molecular signal transduction pathway for ALI induced by circulating eEVs, Western blot analysis was performed on lung tissues from mice. We observed markedly activated phosphorylation of JAK2/3/STAT3, and extension of IRF-1 with iNOS expression in C57 mice intravenously injected with eEVs alone (Figure 4A–D). Immunofluorescence staining showed that overexpression of phosphorylated JAK2 or JAK3 was colocalized with CD31, a marker of pulmonary endothelial cells (Figure S14 in Supporting Information), consistent with the distribution of eEVs as shown in Figure 1J. Compared to wild-type mice in response to eEVs, we detected decreased phosphorylation of JAK3 and STAT3 but not of JAK2 along with downregulation of IRF-1 extension as well as iNOS expression in TLR4$^{-/-}$ mice (Figure 4A and B). As predicted, we observed enhanced phosphorylation of JAK2/3/STAT3 and IRF-1 extension, but without iNOS expression, after eEV injection in iNOS$^{-/-}$ mice (Figure 4A and C). Further, pretreatment with AG490 abrogated the enhanced phosphorylation of JAK2/3/STAT3 and IRF-1 extension as well as blocked iNOS expression in C57 mice after exposure to eEVs. Furthermore, we detected an enhancement of phosphorylated JAK2/3, but not increased phosphorylation of STAT3, IRF-1 extension, and iNOS expression in wild-type mice pretreated with S3I-201 (Figure 4A and D).

## Enhancement of cytokine/chemokine levels in the lungs of mice induces intrapulmonary immune inflammatory cell aggregation, initiating early acute lung injury

Corresponding with the activation of innate immune sig-

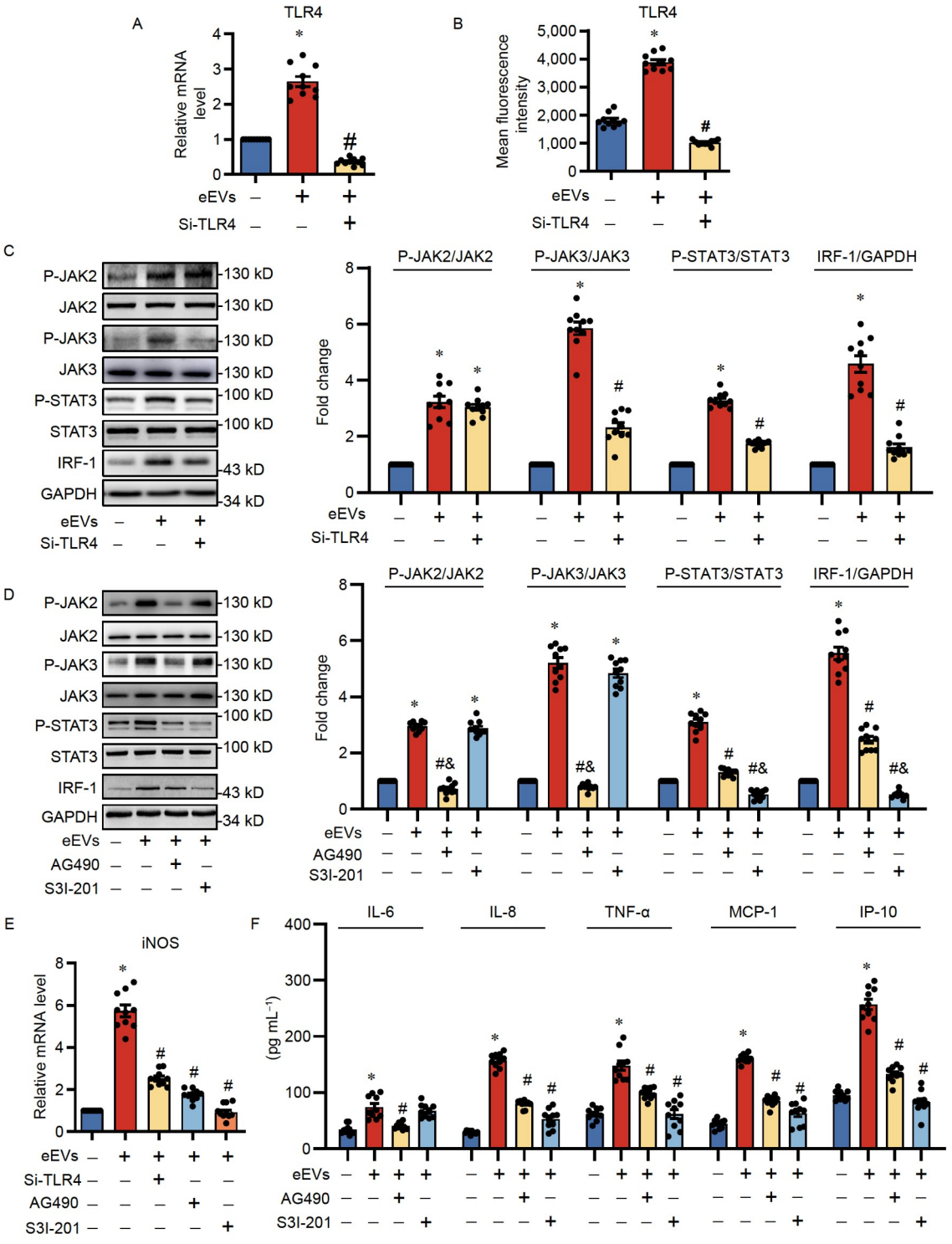


**Figure 2** TLR4-mediated-JAK3/STAT3/IRF-1 signaling activation with cytokine/chemokine secretion in ECs stimulated with eEVs. A and B, The HUVECs were exposed to eEVs with and without Si-TLR4 addition. The HUVECs were treated with starvation medium (0.5% exo-depleted FBS) without eEV addition in the control group. The expression of TLR4 in HUVECs was detected using quantitative real-time reverse transcription polymerase chain reaction and flow cytometry. C, Phosphorylated/non-phosphorylated JAK2, JAK3, and STAT3, and IRF-1 tested using Western blot and quantification analysis in eEVs-exposed HUVECS with and without Si-TLR4 addition. D, Western blot and quantification analysis showing the expression of phosphorylated/non-phosphorylated JAK2/3 and STAT3 combined with IRF-1 levels in HUVECs exposed to eEVs with and without either AG490 or S3I-201, and in HUVECs treated with starvation medium as a control. E, mRNA levels of iNOS in eEV-exposed HUVECs with and without Si-TLR4 addition, AG490 or S3I-201. F, Liquid chromatography showing the levels of cytokine/chemokine in supernatants of eEV-stimulated HUVECs with or without AG490 or S3I-201 addition. All data represent the mean and SEM of independent experiments. Statistical analysis was performed using one-way ANOVA with Tukey's test for panels A–F. (Si-TLR4, silencing TLR4; IL-6, interleukin-6; IL-8, interleukin-8; TNF-α, tumor necrosis factor-α; MCP-1, monocyte chemotactic protein-1. *vs*. Control; # *vs*. eEVs; & *vs*. eEVs plus S3I-201 or AG490. $P<0.05$, $n=10$).

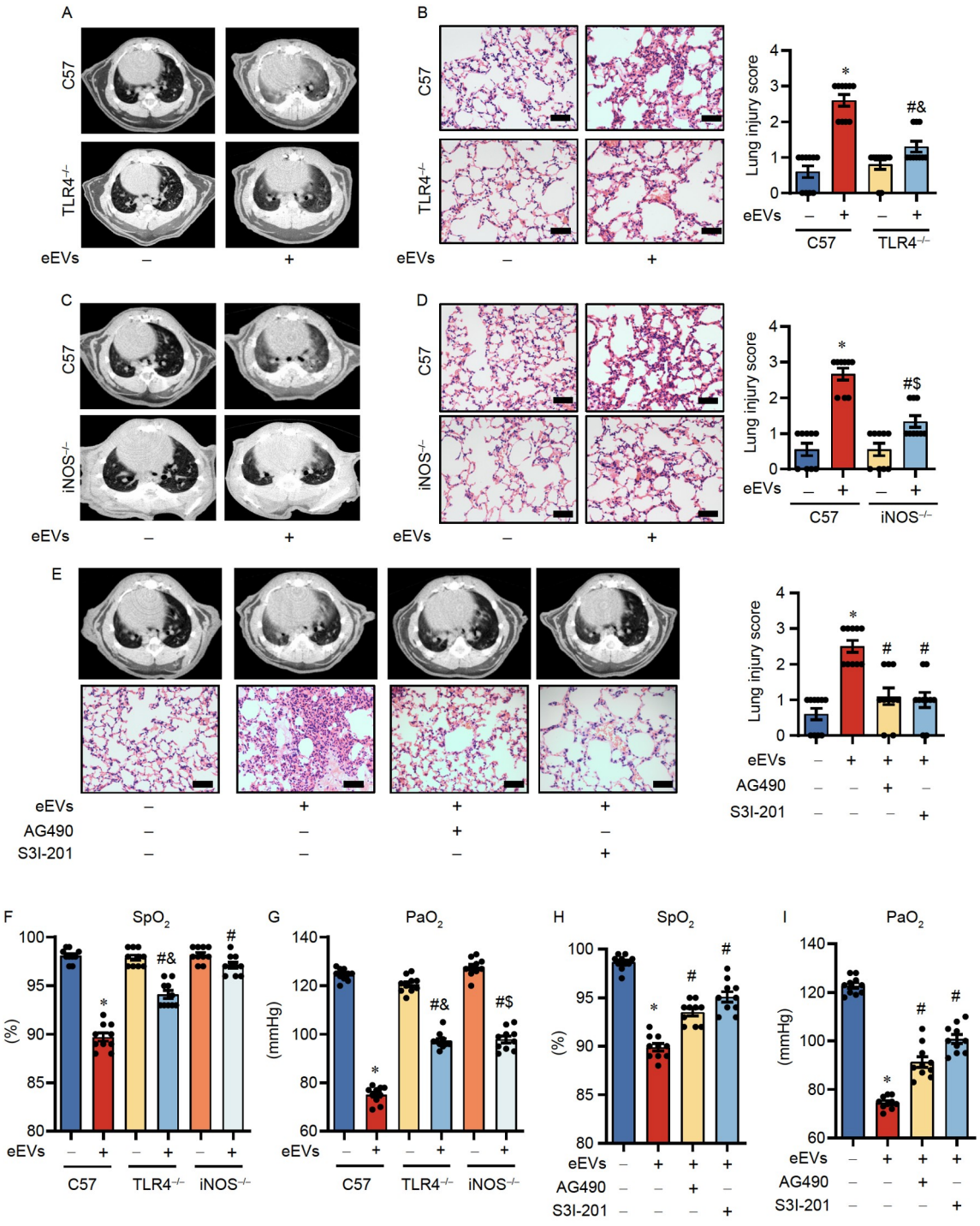


**Figure 3** Impact of eEVs on ALI in C57, TLR4$^{-/-}$ and iNOS$^{-/-}$ mice. A and B, Comparison of lung micro-CT images and H&E staining with lung injury scores of the lung sections in C57 or TLR4$^{-/-}$ mice before and after eEVs instillation. The C57 or TLR4$^{-/-}$ mice were injected with saline in the same volume as eEVs in the control group. C and D, Micro-CT lung images and H&E staining with lung injury score of the lung tissue sections in C57 or iNOS$^{-/-}$ mice with or without eEV treatment. C57 or iNOS$^{-/-}$ mice were injected with saline at the same volume as eEVs in the control group. E, Lung micro-CT images and H&E staining with lung injury scores of lung tissue sections in C57 mice pretreated with AG490 or S3I-201 or saline for 2 h prior to eEV intravenous injection, and in control C57 mice treated with saline without eEV addition. F–I, $PaO_2$ and $SpO_2$ were detected using the blood-gas analyzer in C57, TLR4$^{-/-}$, and iNOS$^{-/-}$ mice before and after eEV injection, and in C57 mice pretreated with AG490 or S3I-201 before eEV intravenous injection. All data represent the mean and SEM of independent experiments. Statistical analysis was performed using one-way ANOVA with Tukey's test for panels B, D, and E–I. (Scale bars: 50 μm. **vs*. C57 negative control; # *vs*. C57 treated with eEVs; & *vs*. TLR4$^{-/-}$ negative control; $ *vs*. iNOS$^{-/-}$ negative control. $P$<0.05, $n$=10).

naling as described above, our data showed elevated cytokine/chemokine levels in plasma/bronchoalveolar lavage fluid (BALF) and aggregation of immune cells, including lymphocytes and neutrophils, in the pulmonary bronchial

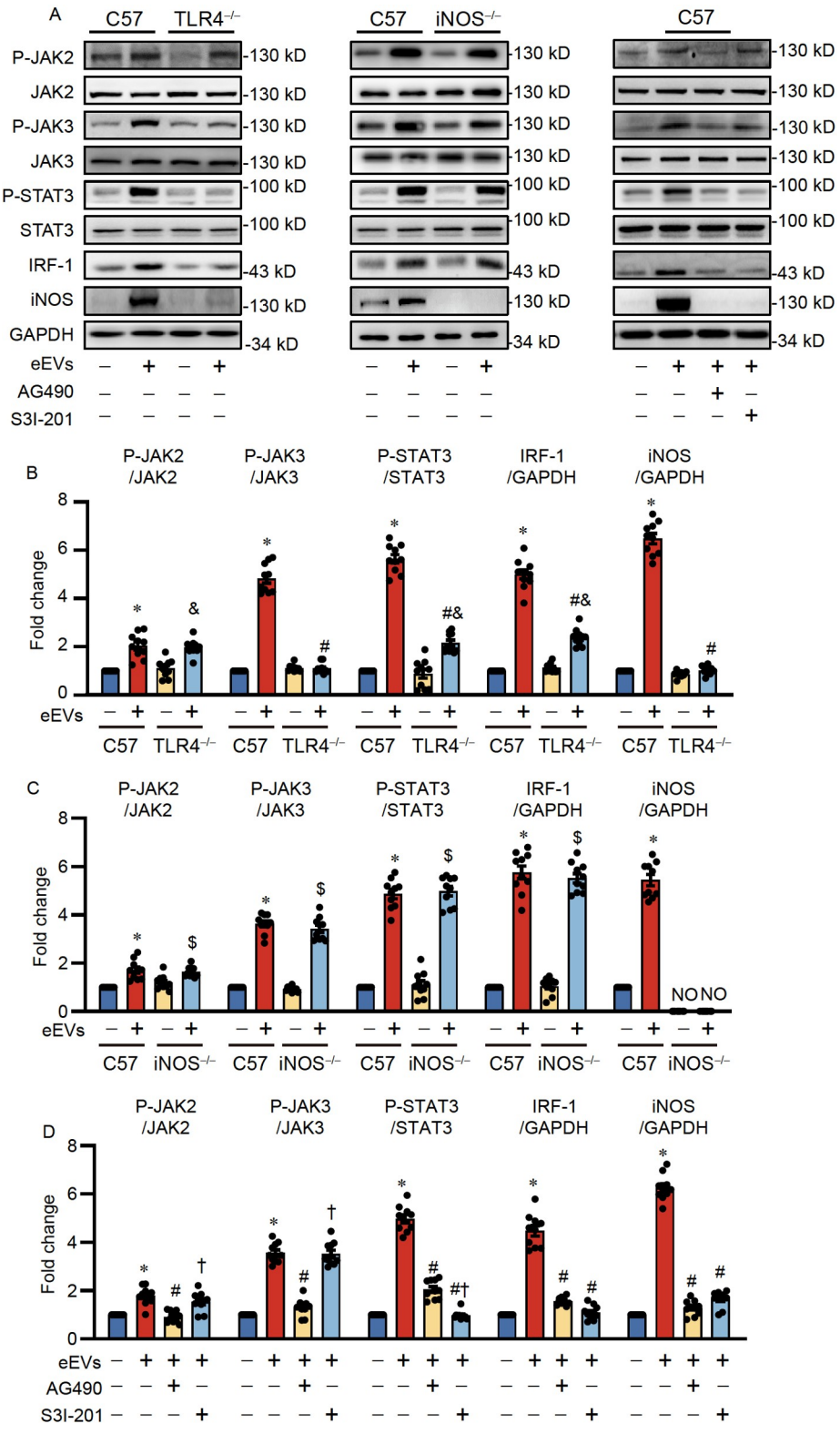


**Figure 4** Investigation of JAK2/3/STAT3/IRF-1/iNOS signaling after eEV exposure in C57, TLR4$^{-/-}$ and iNOS$^{-/-}$ mice. A, Western blots showing the expression of phosphorylated/non-phosphorylated JAK2/3 and STAT3, as well as IRF-1 and iNOS in lung tissues of C57, TLR4$^{-/-}$ and iNOS$^{-/-}$ mice before and after eEV instillation, and in the C57 mice pretreated with AG490 or S3I-201 before eEV intravenous injection. C57, iNOS$^{-/-}$, or TLR4$^{-/-}$mice were injected with saline at the same volume as eEVs in the control groups. B–D, Comparison of JAK2/3/STAT3/IRF-1 signal transduction and iNOS expression in the treated mice as described above in their lung tissues. All data represent the mean and SEM of independent experiments. Statistical analysis was performed using one-way ANOVA with Tukey's test for panels B–D. (**vs*. C57 negative control; # *vs*. C57 treated with eEVs; & *vs*. TLR4$^{-/-}$ negative control; $ *vs*. iNOS$^{-/-}$ negative control; † *vs*. eEVs plus AG490. NO, no expression. $P$<0.05, $n$=10).

alveoli of C57 mice intravenously injected with eEVs (Figure 5).

Lower levels of cytokines/chemokines were detected in the plasma and BALF of TLR4$^{-/-}$ mice than in those of C57 mice after eEV injection (Figure 5A and B; Figure S15A and B in Supporting Information). We also showed that the levels of interleukin-6 (IL-6), tumor necrosis factor-α (TNF-α), and interferon-γ (IFN-γ) released into plasma or BALF were lower in iNOS$^{-/-}$ mice than in C57 mice after exposure to eEVs (Figure 5A and B; Figure S15A and B in Supporting Information). Although the remarkable elevation of the chemokines, IP-10 and monocyte chemotactic protein-1 (MCP-1), was partly decreased in the BALF, they were not reduced in the plasma of iNOS-deleted mice compared with those in C57 mice after eEV injection (Figure 5A and B; Figure S15A and B in Supporting Information). The marked aggregation of immune cells, including lymphocytes and neutrophils, in the pulmonary bronchial alveoli of C57 mice after eEVs injection was inhibited in eEV-injected TLR4$^{-/-}$ mice (Figure 5C and D). We showed that in eEV-treated iNOS$^{-/-}$ mice, there was a marked increase in the level of BALF neutrophils compared to that in eEV-challenged C57 mice as well as that in iNOS$^{-/-}$ mice without eEVs (Figure 5E and F), which was correlated with the high levels of BALF/plasma chemokines, IP-10 and MCP-1, following eEV injection (Figure 5A and B). iNOS deletion in mice did not decrease the induction of large numbers of lymphocytes in BALF owing to the addition of eEVs, but the total number of cells and monocytes were lower in iNOS$^{-/-}$ mice than in wild-type mice (Figure 5E and F).

Wild-type mice pretreated with either AG490 or S3I-201 showed significantly reduced cytokine/chemokine levels, as well as the number of BALF lymphocytes/neutrophils following eEV injection, compared with those in C57 mice pretreated with eEVs (Figure 5G–J; and Figure S15C and D in Supporting Information).

### eEVs carry and transfer FSTL1 targeted toward TLR4 expressed on vascular endothelial cells to trigger the TLR4 downstream signaling pathway-JAK3/STAT3/IRF-1, primarily contributing to ALI

As predicted (Figure S16A in Supporting Information), several protein components of eEVs, including galectin-3 (LGALS3), heat shock 70 kD protein, beta-2-microglobulin (B2M), annexin A5, FSTL1, and alpha-enolase (ENO-1), could be involved in the linkage with TLR4. We detected these components in non-stimulated HUVECs, PAI-1-stimulated HUVECs, eEVs controls, and PAI-1-generated eEVs. We found that the content of FSTL1 harvested from PAI-1-generated eEVs was significantly higher than that from eEV controls (Figure 6A and B). Using a co-immunoprecipitation (Co-IP) assay, we demonstrated that TLR4 can crosslink with B2M, ENO-1, and LGALS3 in cultured HUVECs pretreated with or without eEVs (Figure 6C). The cross-linking did not show apparent discrepancies after eEV pretreatment (Figure 6C). However, we could not detect a linkage between FSTL1 and TLR4 in HUVECs without eEV stimulation, whereas we did observe a definite cross-linkage between them in cells challenged by eEVs (Figure 6C and D).

Furthermore, we showed significantly decreased TLR4 expression in eEV$^{Si\text{-}FSTL1}$ (eEVs derived from HUVECs pretreated with Si-RNA-targeted FSTL1)-treated HUVECs, accompanied by the blockade of phosphorylated JAK3 and STAT3, as well as IRF-1 extension, compared to that in the eEV$^{Si\text{-}C}$ (eEVs derived from HUVECs pretreated with Si-RNA control)-treated cells (Figure 6E and F), while addition of eEV$^{Si\text{-}FSTL1}$ did not induce elevation of cytokine/chemokine production that was observed in eEV$^{Si\text{-}C}$-challenged HUVECs (Figure 6G). *In vivo*, micro-CT scans and pulmonary pathological examination provided evidence showing significantly decreased ALI in wild-type mice after intravenous injection with eEV$^{Si\text{-}FSTL1}$, compared with that in mice injected with eEV$^{Si\text{-}C}$ (Figure 6H and I). Similarly, intravenous addition of lysed eEVs did not effectively induce ALI (Figure S16B in Supporting Information), suggesting the need for intact eEVs as delivering carriers in circulation to transfer FSTL1 targeted toward TLR4.

## DISCUSSION

Secondary inflammatory responses are vital in ALI, and may be attributed to an increase in eEVs (Cabrera-Benítez et al., 2015; Takei et al., 2019; Zhu et al., 2017), which usually occurs during CPB, surgery, toxicity, infection, and trauma (Li et al., 2021; Ma et al., 2021). In the present study, we revealed for the first time that elevated PAI-1 during CPB stimulates the release of eEVs to transfer FSTL1 to vascular ECs by engaging with TLR4 located in the cytomembrane to promote intracellular JAK2/3/STAT3/IRF-1 innate immune inflammatory signal transduction, leading to ALI/ARDS. AG490, an inhibitor of JAK2/3, and S3I-201, an inhibitor of STAT3, can block excessive oxidative stress and cytokine/chemokine storm attacks, thereby preventing the occurrence of ALI/ARDS.

Previous studies have shown that PAI-1 is elevated approximately 15-fold 2 h after cardiac surgery, lasting for the first day after cardiac surgery (Chandler and Velan, 2003). PAI-1 is also increased in ALI, and increasing PAI-1 levels in pulmonary edema fluid and plasma are associated with mortality in patients with ARDS (Ozolina et al., 2016; Prabhakaran et al., 2003). Our data also demonstrate that plasma PAI-1 levels are increased after CPB. Indeed, we found that plasma PAI-1 levels increased more in patients

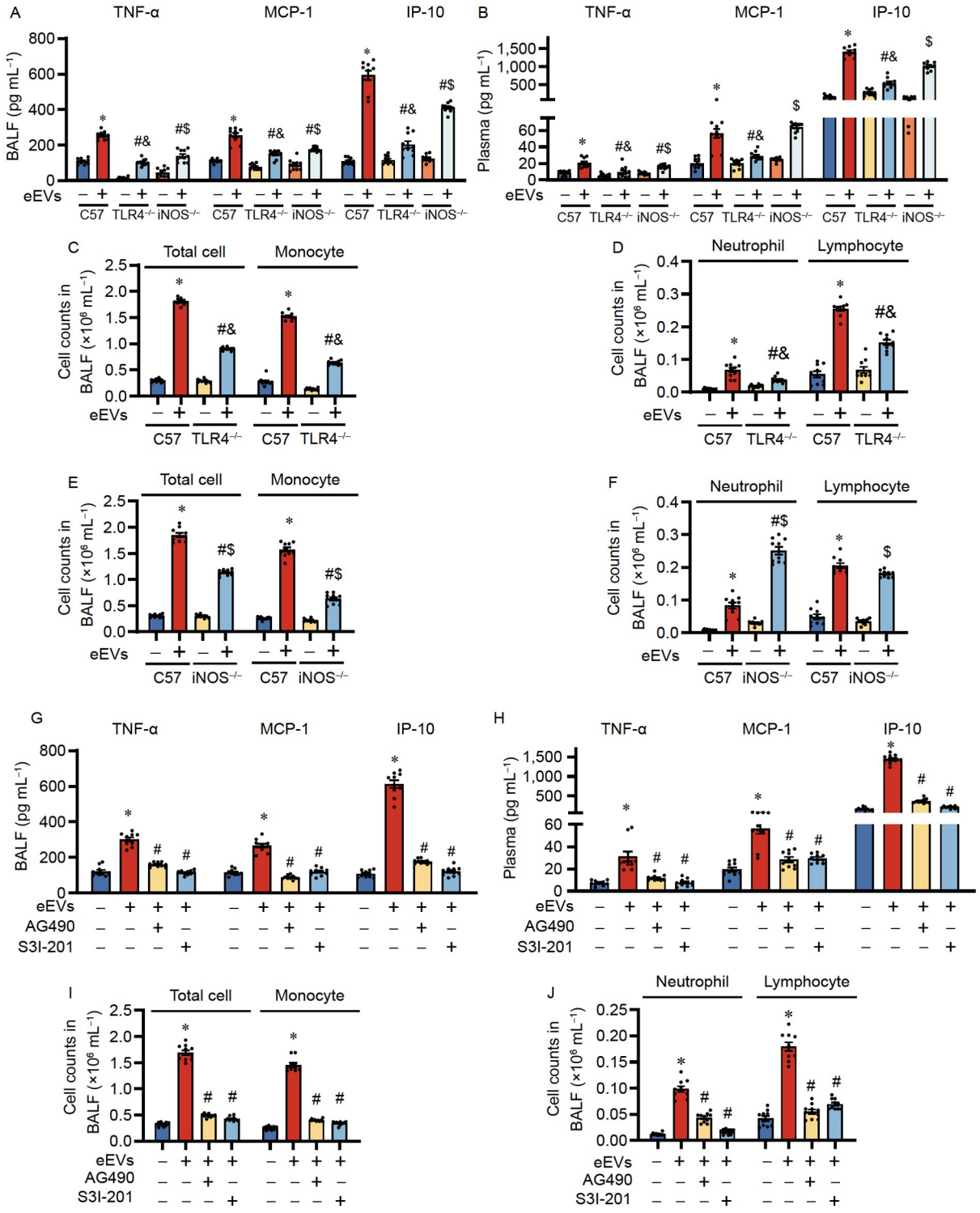


**Figure 5** Comparison of cytokines/chemokines and intrapulmonary immune cell accumulation among different mice stimulated with eEVs. A and B, The levels of TNF-α, MCP-1, and IP-10 in plasma and BALF from the C57, TLR4$^{-/-}$ and iNOS$^{-/-}$ mice before and after eEV injection. C57, iNOS$^{-/-}$, or TLR4$^{-/-}$ mice were injected with saline at the same volume as eEVs in the control groups. C and D, C57 and TLR4$^{-/-}$ mice were intravenously injected with eEVs or saline. The total cell counts and differential cell counts including monocytes, neutrophils, and lymphocytes in the BALF collected from both mice were determined using Wright-Giemsa staining. E and F, The total cell counts and differential counts in the BALF of C57 and iNOS$^{-/-}$ mice at 6 h after eEV administration. G and H, The levels of TNF-α, MCP-1, and IP-10 in plasma and BALF from C57 mice pretreated with AG490 or S3I-201 before eEV intravenous injection. I and J, C57 mice were pretreated with AG490 or S3I-201 or saline for 2 h prior to eEV intravenous injection and the total and differential cell counts in the BALF collected from the treated mice were determined. Statistical analysis was performed using one-way ANOVA with Tukey's test for panels A–J. (*$vs$. C57 negative control; # $vs$. C57 treated with eEVs; & $vs$. TLR4$^{-/-}$ negative control; \$ $vs$. iNOS$^{-/-}$ negative control. $P$<0.05, $n$=10).

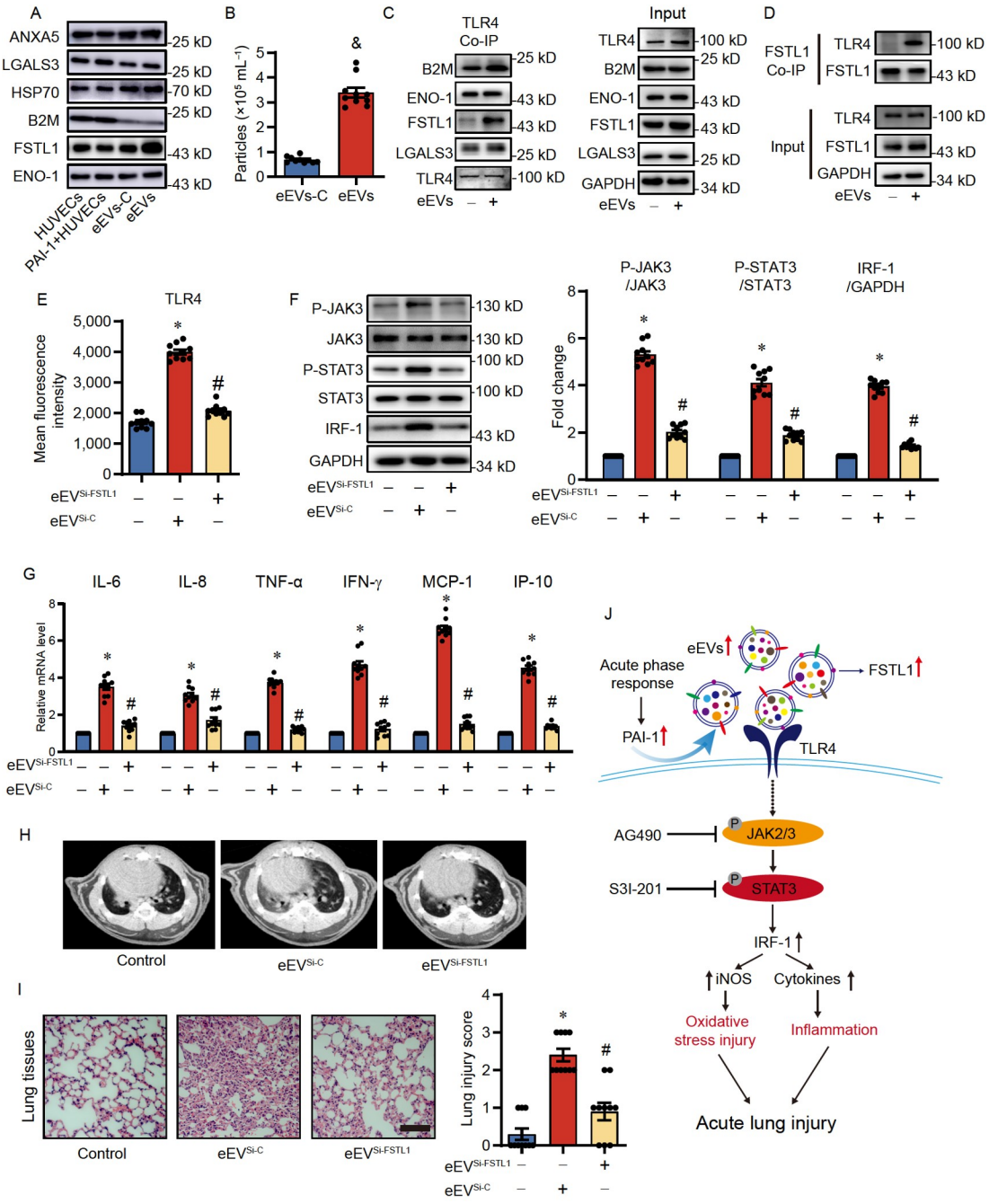


**Figure 6** FSTL1 enclosed in eEVs is responsible for crosstalk with TLR4 in ECs leading to ALI. A, Protein components of LGALS3, heat shock 70 kD protein (HSP70), B2M, annexin A5 (ANXA5), FSTL1, and ENO-1 in HUVECs, PAI-1-treated HUVECs, eEVs-C (eEVs derived from HUVECs), and eEVs (eEVs derived from PAI-1-treated HUVECs) were determined using Western blots. B, Concentrations of eEVs and eEVs-C in the supernatants of HUVECs treated with and without PAI-1. C, Detectable protein components of input-immunoprecipitation and those pulled down by TLR4-Co-IP in extracts from HUVECs plus eEVs or HUVECs alone (without eEVs addition). D, Expression of TLR4 and FSTL1 in the proteins pulled down by FSTL1-Co-IP and input-immunoprecipitation in HUVECs stimulated with or without eEVs (right). E, The expression of "TLR4+" HUVECs treated with $eEV^{Si\text{-}FSTL1}$ (eEVs derived from HUVECs pretreated with Si-RNA targeted to FSTL1) or $eEV^{Si\text{-}C}$ (eEVs derived from HUVECs pretreated with Si-RNA control) or starvation medium (0.5% exo-depleted FBS) without eEV addition for 12 h prior to flow cytometry analysis. F, Phosphorylation of JAK3 and STAT3, and expression of IRF-1 in HUVECs exposed to $eEV^{Si\text{-}FSTL1}$ or $eEV^{Si\text{-}C}$ and in HUVECs stimulated with the starvation medium alone. G, mRNA levels of cytokines/chemokines in HUVECs stimulated with or without $eEV^{Si\text{-}FSTL1}$ or $eEV^{Si\text{-}C}$ for 6 h prior to RT-qPCR test. H and I, C57 mice were intravenously injected with $eEV^{Si\text{-}FSTL1}$ or $eEV^{Si\text{-}C}$ or saline. Comparison of lung micro-CT images and H&E staining with lung injury scores of lung sections in C57 mice treated with saline or $eEV^{Si\text{-}FSTL1}$ or $eEV^{Si\text{-}C}$ (scale bars: 100 μm). J, Hypothetical working model of eEV-induced ALI. Elevated PAI-1 production, during the CPB procedure in cardiac surgery patients, stimulation of eEV released into circulation to transport the enclosed FSTL1 linking with TLR4 for activation of JAK2/3/STAT3/IRF-1 signaling pathway, resulting in a cytokine/chemokine burst and excessive iNOS induction associated with a secondary lung inflammatory response, which contributes to ALI/ARDS. Targeting the JAK2/3/STAT3 signaling pathway is feasible for preventing eEV-induced ALI. All data represent the mean and SEM of independent experiments. Statistical analysis was performed using the *t*-test for panel B and one-way ANOVA with Tukey's test for panels E–G and I. (& *vs*. eEVs-C; **vs*. control; # *vs*. $eEV^{Si\text{-}C}$. $P<0.05$, $n=10$).

with ALI after cardiac surgery with CPB and were negatively correlated with the oxygenation index after CPB. A prospective case-control study of subjects undergoing thoracic, aortic vascular, or cardiac surgery revealed that patients who developed post-operative ARDS showed higher levels PAI-1, further supporting our findings (Yadav et al., 2018). More importantly, our data showed that plasma eEV levels also increased significantly after CPB. Using the current technology, only total EVs can be isolated from plasma. Subgroups of EVs, including eEVs, platelet EVs, and monocyte EVs, can not be separated during isolation using flow cytometry. Therefore, extraction of eEVs from plasma to perform subsequent experiments is challenging. To study the effects of eEVs on ALI, we isolated eEVs from PAI-1-stimulated endothelial cells to perform other experiments and to mimic the circulating eEVs in the plasma of patients undergoing CPB. In fact, PAI-1, as a classical inducer of eEVs, has been used in our previous studies and in other studies to investigate the pathological mechanisms of endothelial injury and ALI (Buesing et al., 2011; Ci et al., 2013; Densmore et al., 2006; Klinkner et al., 2006; Lin et al., 2017; Ou et al., 2011).

Recently, many studies have shown that cell-derived EVs can be transferred to target cells and influence biological processes via TLR (Qiu et al., 2020). Downstream of TLR4, the JAK/STAT pathway is essential for addressing the diverse challenges faced by the immune system, and exaggerated or protracted JAK/STAT signaling has been implicated in most autoimmune diseases and in immune-associated pathological situations such as ischemia-reperfusion injury and systemic inflammatory response syndrome (Hu et al., 2021; Xin et al., 2020). We have previously demonstrated that exposure to hemagglutinin (HA), the surface glycoprotein of the H5N1 virus, stimulated the activation of IFN-independent JAK/STAT and nuclear factor-kappa B (NF-κB) in pulmonary epithelial cells. JAK3 is a molecular determinant of the H5N1 HA-induced dysregulated innate immune response (Cao et al., 2015; Xu et al., 2012). With the suppression of JAK3, pretreatment JAK3 inhibitor suppressed HA-induced phosphorylation of NF-κB to reduce the release of pro-inflammatory cytokines such as IL-6, IL-8, MCP-1, and IP-10 *in vitro* (Cao et al., 2015). As JAK3-dependent signals affect NF-κB transcriptional activation, we focused on the JAK-STAT signaling pathway in eEV-induced lung injury.

FSTL1, a secreted glycoprotein, is widely expressed in human and mouse tissues, but its expression is restricted to cells of the non-hematopoietic lineage (Benedikter et al., 2017). Increasing evidence has shown that the concentration of FSTL1 in circulation shifts during pathological conditions, affecting individual cell behaviors such as proliferation and migration, as well as participating in paracrine communication between cells, inflammation, and vascularization (Fang et al., 2017; Loh et al., 2021; Mattiotti et al., 2018; Peters et al., 2019; Wang et al., 2021). FSTL1 has been observed to have a dual function during inflammatory diseases, acting as an anti-inflammatory factor in the acute phase but having a pro-inflammatory effect in the long term and in chronic diseases (Mattiotti et al., 2018). The present data show that FSTL1 is responsible for eEV-associated ALI, providing the first *in vivo* demonstration of the importance of its role in inducing pulmonary acute inflammatory injury. Consistent with our findings showing attenuation of ALI/ARDS in mice treated with FSTL1-knockdown eEVs, overexpression of FSTL1 in a septic shock mouse model was reported to induce FSTL1-mediated pro-inflammatory events (Chaly et al., 2014). Moreover, stimulation of nucleus pulposus cells with TNF-α was found to induce FSTL1 secretion, indicating a positive feedback loop in the inflammatory response (Liu et al., 2017). However, the mechanism by which extracellular FSTL1 exerts its inflammatory event-inducing effect with respect to a positive feedback loop in secondary lung damage remains unclear. Herein, we show that extracellular FSTL1, as a protein cargo delivered by circulating eEVs, can be captured by endothelial TLR4 to trigger an innate immune inflammatory reaction in the pulmonary microcirculation system. The current study opens up a key avenue for understanding eEV-induced lung injury and systemic inflammatory response syndrome, which are attributed to a secondary inflammatory attack.

Oxidative stress and inflammatory responses are widely acknowledged as primary mechanisms leading to ALI. iNOS can generate large amounts of nitric oxide, which can increase pulmonary vascular permeability and induce lung edema (Golden et al., 2021). In the present study, iNOS deficiency partially reduced murine lung inflammation. However, eEV-promoted iNOS induction was obviously regulated by the upstream JAK2/3/STAT3/IRF-1 signal transduction. Blockade of either JAK2/3 or STAT3 using a targeted preparation, as well as TLR4 knockdown, significantly alleviated oxidative stress damage and pulmonary inflammatory cell infiltration, along with attenuated iNOS overexpression and a cytokine/chemokine storm in response to eEVs both *in vivo* and *in vitro*.

There is much evidence indicating the important role of iNOS in eEV-induced pathological processes (Antunes et al., 2021; Bugueno et al., 2020). Additionally, our results also prove that iNOS induction caused by an increase in circulating eEVs is involved in oxidative stress injury to the lung, and that shutting down iNOS plays a role in dealing with ALI. Other researchers (Laubach et al., 1995) and we have shown that neutrophils in $iNOS^{-/-}$ mice infiltrate the lungs more readily under septic or eEV-exposed conditions. In addition, remarkably high levels of plasma/BALF chemokines, IP-10 and MCP-1, are closely correlated with

continuing high levels of lymphocyte migration into the lung, regardless of iNOS deficiency. Thus, iNOS, as a pharmaceutical target, may not be beneficial in clinical practice.

Our findings corroborate that over-activation of the JAK2/3/STAT3 pathway is a common signaling mechanism contributing to the pathogenesis of ALI related to a hyperactive immune response caused by eEV challenge. Furthermore, JAK2/3/STAT3 activation in the lung occurs long before diffuse lung injury is visible, suggesting that JAK2/3/STAT3 signaling plays a central role in early inflammatory cell infiltration and oxidative stress. Additionally, based on our present data, extracellular FSTL1 exerts its pro-inflammatory cytokine-inducing effect through activation of TLR4-mediated JAK3/STAT3 signaling via circulating eEVs delivery. Therefore, elevation of eEVs combined with a high level of cytokines/chemokines in circulation should become an important biomarker for potential hyperactive immune inflammatory hits.

More importantly, in addition to being an intercellular signaling pathway that regulates the expression of target genes, JAK/STAT-specific therapeutics are rapidly being developed to treat autoimmune diseases in the clinic (Matsuyama et al., 2020; Xin et al., 2020). Therefore, we suggest that the JAK2/3/STAT3 pathway should be considered a target for pharmaceuticals in the prevention and/or treatment of secondary inflammation associated with eEV propagation caused by cardiac surgery with CPB.

To our knowledge, the current study demonstrates for the first time that elevated PAI-1 stimulates the release of eEVs to deliver extracellular FSTL1 to TLR4 located in the pulmonary microvascular endothelium, mediating a crosstalk between them for activating innate immune receptor signaling, thus contributing to the extensiveness of the inflammatory response in the pulmonary interstitium. Acute injury of the alveolar membrane induces pulmonary edema and a diffusion disorder, and decreased surfactant production by epithelial cells leads to diffuse microatelectasis, functional shunting, and inflammation causing bronchospasm, vasoconstriction, and thrombosis, which could result in shunting and dead space-like ventilation. All these processes are involved in the pathogenesis of hypoxemia in the early stages of ARDS. In this study, we propose a novel viewpoint that FSTL1 derived from ECs exerts its effects via eEVs to activate TLR4-mediated JAK2/3/STAT3/IRF-1 signaling, leading to ALI (Figure 6J). Moreover, our findings provide new insights into the clinical implementation of pathway-specific therapeutics targeting JAK2/3 using the currently available JAK inhibitors (Figure 6J). As the kinase domains of JAKs are clear pharmacological targets, AG490 and S3I-201 can be considered beneficial for managing eEV-associated ARDS after CPB in clinical management.

## LIMITATIONS

In the present study, we used eEVs generated from human ECs, but not from mouse ECs, to perform experiments in a mouse model. This may cause foreign-body effects in mice. However, using eEVs derived from human ECs can better simulate the pathogenesis of ALI in humans because the components in these eEVs are similar to those in the ALI induced after CPB in patients. The eEV components may differ between humans and mice. Therefore, we selected eEVs from human ECs to study ALI in a mouse model in the present study.

## MATERIALS AND METHODS

Please refer to the online supplement for additional details on the methodology.

### Study population

This study complied with the Declaration of Helsinki of 1975 (as revised in 2008) and was approved by the Ethics Review Board of The First Affiliated Hospital, Sun Yat-sen University ([2011]14). Written informed consent was obtained from all subjects recruited for this study. Patients who underwent cardiac surgery, including valve surgery and coronary artery bypass graft through median sternotomy with CPB, were recruited for the study. The exclusion criteria were age ⩽18 years, previous cardiopulmonary surgery, previous lung disease, renal failure, and hepatic dysfunction. Forty patients undergoing cardiac surgery with CPB were enrolled from The First Affiliated Hospital, Sun Yat-sen University. The levels of plasma PAI-1 and circulating eEVs were measured before and after CPB (Coumans et al., 2017; Royo et al., 2020).

### Experiments on eEV-stimulated endothelial cells

eEVs were isolated from PAI-1-stimulated HUVECs as previously described (Lin et al., 2017). HUVECs were obtained from ScienCell (USA). The phosphorylation/non-phosphorylation of JAK1/2/3 and the expression of STAT1/2/3, IRF-1, iNOS, TLR4, and IP-10 in HUVECs after incubation with eEVs were detected. The levels of IL-6, interleukin-8 (IL-8), MCP-1, TNF-α, and IP-10 were measured in the supernatants of HUVECs treated with eEVs.

HUVECs were treated with silencing TLR4 RNA (Si-TLR4) prior to the addition of eEVs or with AG490 or S3I-201 (inhibitors of JAK (JAK2/3) and STAT3, respectively) for 2 h before eEV stimulation. HUVECs were treated with starvation medium (0.5% exo-depleted FBS) without eEVs in the control groups. HUVECs were then subjected to the

measurements described above.

Co-immunoprecipitation and Western blot analyses were performed to identify the proteins in the eEVs and their binding abilities with TLR4 in HUVECs. Next, HUVECs were treated with $eEV^{Si\text{-}FSTL1}$ derived from HUVECs pretreated with siRNA for knockdown of FSTL1 or with $eEV^{Si\text{-}C}$ (eEVs derived from HUVECs pretreated with siRNA control). HUVECs were treated with starvation medium (0.5% exo-depleted FBS) without $eEV^{Si\text{-}FSTL1}$ or with $eEV^{Si\text{-}C}$ addition in the control groups. Activation of TLR4/JAK3/STAT3 signaling pathways in HUVECs treated with $eEV^{Si\text{-}FSTL1}$ or $eEV^{Si\text{-}C}$ was detected.

## Animal studies

All animal experiments were approved by the Ethics Review Board and Animal Research Committee of The First Affiliated Hospital, Sun Yat-sen University, and were conducted in accordance with the Guide for the Care and Use of Animals in Research of the People's Republic of China. Eight-week-old male and female C57BL/6 wild-type (C57) mice, $TLR4^{-/-}$ mice, and $iNOS^{-/-}$ mice were obtained from GemPharmatech Co., Ltd., (USA) and the Jackson Laboratory (USA). The eEV-induced ALI procedure was conducted as previously described (Densmore et al., 2006). C57 mice were pretreated with or without AG490 or S3I-201 prior to intravenous injection of eEVs. Saline at the same volume without eEV addition was injected into the C57, $iNOS^{-/-}$, and $TLR4^{-/-}$ mice in the control groups.

After 6 h, the mice were anesthetized with inhaled isoflurane (5% isoflurane and 100% oxygen) for the initial induction and maintained under 2% isoflurane in 100% oxygen throughout the procedure. A lack of response to toe pinching indicates successful anesthesia. Chest micro-CT, $SpO_2$ and $PaO_2$ examinations were performed to assess pulmonary effusion and hypoxemia. The mice were then euthanized to collect BALF for cell and differential counts as well as cytokine measurements; lung tissue sections were prepared for hematoxylin and eosin (H&E) staining, immunohistochemistry, and Western blot analysis. The animals were euthanized by an intraperitoneal injection of a pentobarbital overdose (100 mg $kg^{-1}$) in a small area away from housing and research facilities.

Cytokine and chemokine levels in the plasma and BALF were analyzed using a Luminex assay liquid chip system.

## Statistical analysis

Data are presented as the mean ± standard error of the mean unless otherwise stated. Differences among test groups were determined using analysis of variance (ANOVA) followed by Tukey's test for more than two groups or *t*-test for two groups. For the clinical study, the *t*-test or Wilcoxon rank-sum test was applied to compare continuous values between two groups based on the results of the test for statistical normality. A $\chi^2$ analysis was conducted to compare categorical variables. Correlation was determined using Spearman's correlation analysis. All statistical analyses were performed using the Statistical Package for Social Sciences (SPSS version 22.0), and *P*-values <0.05 were considered significant.

**Compliance and ethics** *The author(s) declare that they have no conflict of interest. The human and animal studies were approved by the Ethics Review Board of The First Affiliated Hospital, Sun Yat-sen University, and conformed with the Helsinki Declaration of 1975 (as revised in 2008) concerning Human and Animal Rights.*

**Acknowledgements** *This work was supported by the National Key Research and Development Program of China (2021YFA0805100), the National Natural Science Foundation of China (81830013, 81770241, 81970363, 82000362, 92268202, 81170271, 81370370, 81490531, 81670392, 81600382), the National Natural Science Foundation of China Distinguished Young Scholar Grant (81325001), "973 Project" from the Ministry of Science and Technology of China (2009CB522104), Guangdong Basic and Applied Basic Research Foundation, China (2019B1515120092), the Science and Technology Planning Project of Guangzhou, China (202103000016), the Changjiang Scholars Program from the Ministry of Education of China, the Sun Yat-sen University Clinical Research 5010 Program, and the Program of National Key Clinical Specialties. The authors would like to thank Jian Ma, Ze-Bang Lin, and the staff at The First Affiliated Hospital, Sun Yat-sen University, and Guangzhou Institute of Respiratory Health for their assistance throughout this study.*

## References

Andres, J., Smith, L.C., Murray, A., Jin, Y., Businaro, R., Laskin, J.D., and Laskin, D.L. (2020). Role of extracellular vesicles in cell-cell communication and inflammation following exposure to pulmonary toxicants. Cytokine Growth Factor Rev 51, 12–18.

Antunes, M.A., Braga, C.L., Oliveira, T.B., Kitoko, J.Z., Castro, L.L., Xisto, D.G., Coelho, M.S., Rocha, N., Silva-Aguiar, R.P., Caruso-Neves, C., et al. (2021). Mesenchymal stromal cells from emphysematous donors and their extracellular vesicles are unable to reverse cardiorespiratory dysfunction in experimental severe emphysema. Front Cell Dev Biol 9, 661385.

Benedikter, B.J., Bouwman, F.G., Vajen, T., Heinzmann, A.C.A., Grauls, G., Mariman, E.C., Wouters, E.F.M., Savelkoul, P.H., Lopez-Iglesias, C., Koenen, R.R., et al. (2017). Ultrafiltration combined with size exclusion chromatography efficiently isolates extracellular vesicles from cell culture media for compositional and functional studies. Sci Rep 7, 15297.

Buesing, K.L., Densmore, J.C., Kaul, S., Pritchard Jr., K.A., Jarzembowski, J.A., Gourlay, D.M., and Oldham, K.T. (2011). Endothelial microparticles induce inflammation in acute lung injury. J Surg Res 166, 32–39.

Bugueno, I.M., Zobairi El-Ghazouani, F., Batool, F., El Itawi, H., Anglès-Cano, E., Benkirane-Jessel, N., Toti, F., and Huck, O. (2020). *Porphyromonas gingivalis* triggers the shedding of inflammatory endothelial microvesicles that act as autocrine effectors of endothelial dysfunction. Sci Rep 10, 1778.

Cabrera-Benítez, N.E., Valladares, F., García-Hernández, S., Ramos-Nuez, Á., Martín-Barrasa, J.L., Martínez-Saavedra, M.T., Rodríguez-Gallego, C., Muros, M., Flores, C., Liu, M., et al. (2015). Altered profile of

circulating endothelial-derived microparticles in ventilator-induced lung injury. Crit Care Med 43, e551–e559.
Cao, K., Chen, M., Jie, X., Wang, Y., Li, Q., and Xu, J. (2015). H5N1 virus hemagglutinin inhibition of cAMP-dependent CFTR via TLR4-mediated janus tyrosine kinase 3 activation exacerbates lung inflammation. Mol Med 21, 134–142.
Chaly, Y., Fu, Y., Marinov, A., Hostager, B., Yan, W., Campfield, B., Kellum, J.A., Bushnell, D., Wang, Y., Vockley, J., et al. (2014). Follistatin-like protein 1 enhances NLRP3 inflammasome-mediated IL-1β secretion from monocytes and macrophages. Eur J Immunol 44, 1467–1479.
Chandler, W.L., and Velan, T. (2003). Secretion of tissue plasminogen activator and plasminogen activator inhibitor 1 during cardiopulmonary bypass. Thromb Res 112, 185–192.
Chen, Y.T., Yuan, H.X., Ou, Z.J., and Ou, J.S. (2020). Microparticles (exosomes) and atherosclerosis. Curr Atheroscler Rep 22, 23.
Ci, H.B., Ou, Z.J., Chang, F.J., Liu, D.H., He, G.W., Xu, Z., Yuan, H.Y., Wang, Z.P., Zhang, X., and Ou, J.S. (2013). Endothelial microparticles increase in mitral valve disease and impair mitral valve endothelial function. Am J Physiol Endocrinol Metab 304, E695–E702.
Coats, T.J., and Morsy, M. (2020). Biological mechanisms and individual variation in fibrinolysis after major trauma. Emerg Med J 37, 135–140.
Coumans, F.A.W., Brisson, A.R., Buzas, E.I., Dignat-George, F., Drees, E. E.E., El-Andaloussi, S., Emanueli, C., Gasecka, A., Hendrix, A., Hill, A.F., et al. (2017). Methodological guidelines to study extracellular vesicles. Circ Res 120, 1632–1648.
Densmore, J.C., Signorino, P.R., Ou, J., Hatoum, O.A., Rowe, J.J., Shi, Y., Kaul, S., Jones, D.W., Sabina, R.E., Pritchard, K.A., et al. (2006). Endothelium-derived microparticles induce endothelial dysfunction and acute lung injury. Shock 26, 464–471.
Fang, Y., Zhang, S., Li, X., Jiang, F., Ye, Q., and Ning, W. (2017). Follistatin like-1 aggravates silica-induced mouse lung injury. Sci Rep 7, 399.
Fujimoto, S., Fujita, Y., Kadota, T., Araya, J., and Kuwano, K. (2020). Intercellular communication by vascular endothelial cell-derived extracellular vesicles and their micrornas in respiratory diseases. Front Mol Biosci 7, 619697.
Golden, T.N., Venosa, A., and Gow, A.J. (2021). Cell origin and inos function are critical to macrophage activation following acute lung injury. Front Pharmacol 12, 761496.
Hu, X., li, J., Fu, M., Zhao, X., and Wang, W. (2021). The JAK/STAT signaling pathway: from bench to clinic. Sig Transduct Target Ther 6, 402.
Jian, Y.P., Yuan, H.X., Hu, K.H., Chen, C., Li, Y.Q., Li, Y., Yang, T.X., Ou, Z.J., and Ou, J.S. (2019). Protein compositions changes of circulating microparticles in patients with valvular heart disease subjected to cardiac surgery contribute to systemic inflammatory response and disorder of coagulation. Shock 52, 487–496.
Kim, J., Baalachandran, R., Li, Y., Zhang, C.O., Ke, Y., Karki, P., Birukov, K.G., and Birukova, A.A. (2022). Circulating extracellular histones exacerbate acute lung injury by augmenting pulmonary endothelial dysfunction via TLR4-dependent mechanism. Am J Physiol Lung Cell Mol Physiol 323, L223–L239.
Klinkner, D.B., Densmore, J.C., Kaul, S., Noll, L.A., Lim, H.J., Weihrauch, D., Pritchard Jr., K.A., Oldham, K.T., and Sander, T.L. (2006). Endothelium-derived microparticles inhibit human cardiac valve endothelial cell function. Shock 25, 575–580.
Kwak, S.Y., Park, S., Kim, H., Lee, S.J., Jang, W.S., Kim, M.J., Lee, S.B., Jang, W.I., Kim, A.R., Kim, E.H., et al. (2021). Atorvastatin inhibits endothelial PAI-1-mediated monocyte migration and alleviates radiation-induced enteropathy. Int J Mol Sci 22, 1828.
Laubach, V.E., Shesely, E.G., Smithies, O., and Sherman, P.A. (1995). Mice lacking inducible nitric oxide synthase are not resistant to lipopolysaccharide-induced death. Proc Natl Acad Sci USA 92, 10688–10692.
Li, Y., Yuan, H., Chen, C., Chen, C., Ma, J., Chen, Y., Li, Y., Jian, Y., Liu, D., Ou, Z., et al. (2021). Concentration of circulating microparticles: a new biomarker of acute heart failure after cardiac surgery with cardiopulmonary bypass. Sci China Life Sci 64, 107–116.
Lin, Z.B., Ci, H.B., Li, Y., Cheng, T.P., Liu, D.H., Wang, Y.S., Xu, J., Yuan, H.X., Li, H.M., Chen, J., et al. (2017). Endothelial microparticles are increased in congenital heart diseases and contribute to endothelial dysfunction. J Transl Med 15, 4.
Liu, Y., Wei, J., Zhao, Y., Zhang, Y., Han, Y., Chen, B., Cheng, K., Jia, J., Nie, L., and Cheng, L. (2017). Follistatin-like protein 1 promotes inflammatory reactions in nucleus pulposus cells by interacting with the MAPK and NFκB signaling pathways. Oncotarget 8, 43023–43034.
Loh, J.J., Li, T.W., Zhou, L., Wong, T.L., Liu, X., Ma, V.W.S., Lo, C.M., Man, K., Lee, T.K., Ning, W., et al. (2021). Fstl1 secreted by activated fibroblasts promotes hepatocellular carcinoma metastasis and stemness. Cancer Res 81, 5692–5705.
Ma, J., Yuan, H.X., Chen, Y.T., Ning, D.S., Liu, X.J., Peng, Y.M., Chen, C., Song, Y.K., Jian, Y.P., Li, Y., et al. (2021). Circulating endothelial microparticles: a promising biomarker of acute kidney injury after cardiac surgery with cardiopulmonary bypass. Ann Transl Med 9, 786.
Matsuyama, T., Kubli, S.P., Yoshinaga, S.K., Pfeffer, K., and Mak, T.W. (2020). An aberrant stat pathway is central to COVID-19. Cell Death Differ 27, 3209–3225.
Mattiotti, A., Prakash, S., Barnett, P., and van den Hoff, M.J.B. (2018). Follistatin-like 1 in development and human diseases. Cell Mol Life Sci 75, 2339–2354.
Ou, Z.J., Chang, F.J., Luo, D., Liao, X.L., Wang, Z.P., Zhang, X., Xu, Y.Q., and Ou, J.S. (2011). Endothelium-derived microparticles inhibit angiogenesis in the heart and enhance the inhibitory effects of hypercholesterolemia on angiogenesis. Am J Physiol Endocrinol Metab 300, E661–E668.
Ozolina, A., Sarkele, M., Sabelnikovs, O., Skesters, A., Jaunalksne, I., Serova, J., Ievins, T., Bjertnaes, L.J., and Vanags, I. (2016). Activation of coagulation and fibrinolysis in acute respiratory distress syndrome: a prospective pilot study. Front Med 3.
Peters, M.M.C., Meijs, T.A., Gathier, W., Doevendans, P.A.M., Sluijter, J.P. G., Chamuleau, S.A.J., and Neef, K. (2019). Follistatin-like 1 in cardiovascular disease and inflammation. Mini Rev Med Chem 19, 1379–1389.
Peterson, D.B., Sander, T., Kaul, S., Wakim, B.T., Halligan, B., Twigger, S., Pritchard Jr., K.A., Oldham, K.T., and Ou, J.S. (2008). Comparative proteomic analysis of PAI-1 and TNF-alpha-derived endothelial microparticles. Proteomics 8, 2430–2446.
Prabhakaran, P., Ware, L.B., White, K.E., Cross, M.T., Matthay, M.A., and Olman, M.A. (2003). Elevated levels of plasminogen activator inhibitor-1 in pulmonary edema fluid are associated with mortality in acute lung injury. Am J Physiol Lung Cell Mol Physiol 285, L20–L28.
Qi, X., Chen, S., He, H., Wen, W., and Wang, H. (2021). The role and potential application of extracellular vesicles in liver cancer. Sci China Life Sci 64, 1281–1294.
Qiu, Q., Yang, Z., Cao, F., Yang, C., Hardy, P., Yan, X., Yang, S., and Xiong, W. (2020). Activation of NLRP3 inflammasome by lymphocytic microparticles via TLR4 pathway contributes to airway inflammation. Exp Cell Res 386, 111737.
Royo, F., Théry, C., Falcón-Pérez, J.M., Nieuwland, R., and Witwer, K.W. (2020). Methods for separation and characterization of extracellular vesicles: results of a worldwide survey performed by the ISEV rigor and standardization subcommittee. Cells 9, 1955.
Sandeep, B., Xiao, Z., Zhao, F., Feng, Q., and Gao, K. (2022). Role of platelets in acute lung injury after extracorporeal circulation in cardiac surgery patients: a systemic review. Curr Probl Cardiol 47, 101088.
Sander, T.L., Ou, J.S., Densmore, J.C., Kaul, S., Matus, I., Twigger, S., Halligan, B., Greene, A.S., Pritchard, K.A., and Oldham, K.T. (2008). Protein composition of plasminogen activator inhibitor type 1-derived endothelial microparticles. Shock 29, 504–511.
Shirey, K.A., Blanco, J.C.G., and Vogel, S.N. (2021). Targeting TLR4 signaling to blunt viral-mediated acute lung injury. Front Immunol 12, 705080.

Song, Y.K., Yuan, H.X., Jian, Y.P., Chen, Y.T., Liang, K.F., Liu, X.J., Ou, Z. J., Liu, J.S., Li, Y., and Ou, J.S. (2022). Pentraxin 3 in circulating microvesicles: a potential biomarker for acute heart failure after cardiac surgery with cardiopulmonary bypass. J Cardiovasc Trans Res 15, 1414–1423.

Takei, Y., Yamada, M., Saito, K., Kameyama, Y., Sugiura, H., Makiguchi, T., Fujino, N., Koarai, A., Toyama, H., Saito, K., et al. (2019). Increase in circulating ACE-positive endothelial microparticles during acute lung injury. Eur Respir J 54, 1801188.

Tipoe, T.L., Wu, W.K.K., Chung, L., Gong, M., Dong, M., Liu, T., Roever, L., Ho, J., Wong, M.C.S., Chan, M.T.V., et al. (2018). Plasminogen activator inhibitor 1 for predicting sepsis severity and mortality outcomes: A systematic review and meta-analysis. Front Immunol 9, 1218.

Wang, Y., Zhang, D., Liu, T., Wang, J., Wu, J., Zhao, J., Xu, J., Zhang, J., and Dong, L. (2021). FSTL1 aggravates OVA-induced inflammatory responses by activating the NLRP3/IL-1β signaling pathway in mice and macrophages. Inflamm Res 70, 777–787.

Xin, P., Xu, X., Deng, C., Liu, S., Wang, Y., Zhou, X., Ma, H., Wei, D., and Sun, S. (2020). The role of JAK/STAT signaling pathway and its inhibitors in diseases. Int Immunopharmacol 80, 106210.

Xu, W., Chen, M., Ge, N., and Xu, J. (2012). Hemagglutinin from the H5N1 virus activates janus kinase 3 to dysregulate innate immunity. PLoS ONE 7, e31721.

Yadav, H., Bartley, A., Keating, S., Meade, L.A., Norris, P.J., Carter, R.E., Gajic, O., and Kor, D.J. (2018). Evolution of validated biomarkers and intraoperative parameters in the development of postoperative ards. Respir Care 63, 1331–1340.

Yuan, H.X., Chen, C.Y., Li, Y.Q., Ning, D.S., Li, Y., Chen, Y.T., Li, S.X., Fu, M.X., Li, X.D., Ma, J., et al. (2020). Circulating extracellular vesicles from patients with valvular heart disease induce neutrophil chemotaxis via FOXO3A and the inhibiting role of dexmedetomidine. Am J Physiol Endocrinol Metab 319, E217–E231.

Yuan, H.X., Liang, K.F., Chen, C., Li, Y.Q., Liu, X.J., Chen, Y.T., Jian, Y.P., Liu, J.S., Xu, Y.Q., Ou, Z.J., et al. (2022). Size distribution of microparticles: a new parameter to predict acute lung injury after cardiac surgery with cardiopulmonary bypass. Front Cardiovasc Med 9, 893609.

Zhu, Q., He, G., Wang, J., Wang, Y., Chen, W., and Guo, T. (2017). Down-regulation of Toll-like receptor 4 alleviates intestinal ischemia reperfusion injury and acute lung injury in mice. Oncotarget 8, 13678–13689.

## SUPPORTING INFORMATION

The supporting information is available online at https://doi.org/10.1007/s11427-022-2328-x. The supporting materials are published as submitted, without typesetting or editing. The responsibility for scientific accuracy and content remains entirely with the authors.